Measurements of a Nonlinear Diocotron Mode in Pure Electron Plasmas

K. S. Fine, C. F. Driscoll, and J. H. Malmberg
Department of Physics, University of California at San Diego, La Jolla, California 92093
(Received 14 August 1989)

Measurements of frequencies and density perturbations of the large amplitude $l=1$, $k_z=0$ diocotron mode on pure electron plasma columns are presented. This mode is a nonlinear dynamical state of an off-axis electron column which is $\mathbf{E}\times\mathbf{B}$ drifting around the containment axis. At large amplitudes, the plasma column distorts into an oval cross section and the mode frequency shifts by an amount proportional to mode amplitude squared. The frequency shift arises because (1) the plasma is closer to its image than a linear model assumes, and (2) the shape distortion modifies the image charge distribution.

PACS numbers: 52.35.Mw, 52.25.Wz

A magnetized pure electron plasma column contained inside conducting cylinders supports electrostatic models that vary as $\exp(il\theta+ik_z z-i\omega t)$. Here we consider the fundamental "diocotron" mode with $l=1$ and $k_z=0$. At large amplitudes, this mode is best described as a stable, nonlinear dynamical state rather than as a perturbation of the type treated by linear theory. The dynamical state is a displaced and distorted electron column which is $\mathbf{E}\times\mathbf{B}$ drifting around the axis of the containment cylinders. Nonlinear effects cause the distortion of the displaced plasma column and a shift in the mode frequency. In this Letter, we present measurements of the density and frequency of this nonlinear state, and find that much of the behavior can be explained with remarkably simple models.

Diocotron modes are found in many magnetized charge-particle systems, such as electron beams,[1] magnetrons,[2] and Penning traps.[3] In many systems, the particle motion along the magnetic field is largely decoupled from these modes: For our system the axial bounce time ($\tau_b\sim 1$ μs) is small compared to the wave period ($1/f\sim 20$ μs), so only the r-θ drift dynamics need to be considered.

The $l=1$, $k_z=0$ mode is unique in that it is an essentially undamped center-of-mass motion in the r-θ plane. Experimentally, we observe no damping in 10^5 cycles, in contradiction to current theory,[4] which generally predicts damping in 10^3 cycles or less. Previous experiments did measure damping of the mode, but this was apparently due to plasma confinement limitations.[5] However, even in perfectly confined plasmas, shear is necessarily present in the drift velocity field at large amplitudes, so the mode may damp on the viscosity time scale of about 10^6 cycles;[6] this has not been treated experimentally or theoretically.

The pure electron plasmas are contained in cylindrical geometry, as shown schematically in Fig. 1. A uniform axial magnetic field B_z provides radial confinement, and negative voltages applied to end cylinders A and C confine the electrons inside the grounded cylinder B. The apparatus is operated in an inject-manipulate-dump cycle. For injection, cylinder A is briefly grounded, allowing electrons to enter from the negatively biased thermionic source. The trapped electrons can then be manipulated, and waves can be transmitted and received using isolated sections of the cylindrical wall. Finally, the plasma is dumped by grounding cylinder C: The electrons stream out along the magnetic field lines, and measurement of the charge Q which passes through the collimator hole of area $A_h=\pi(1.6\text{ mm})^2$ gives the z-averaged electron density

$$n(r,\theta,t)=\frac{Q(r,\theta,t)}{-eA_hL_p}=\frac{1}{L_p}\int dz\,\tilde{n}(r,\theta,z,t)\,.$$

We neglect the 5% variation in plasma length L_p by presuming L_p is constant with radius. The plasmas studied here have density $n\sim 5\times 10^6$ cm^{-3}, thermal energy $kT\sim 1$ eV, radii $1.3<R_p<2.9$ cm, and length $L_p\approx 36$ cm. The cylindrical wall has radius $R_w=3.81$ cm and B_z is 375 G.

Linear theory[7-9] describes the $l=1$, $k_z=0$ diocotron mode as perturbation charges varying as

$$\delta n(r,\theta,t)=-D\frac{dn_0}{dr}e^{i(\theta-2\pi f_0 t)}\,, \qquad (1)$$

propagating on a symmetric plasma $n_0(r)$, where D is

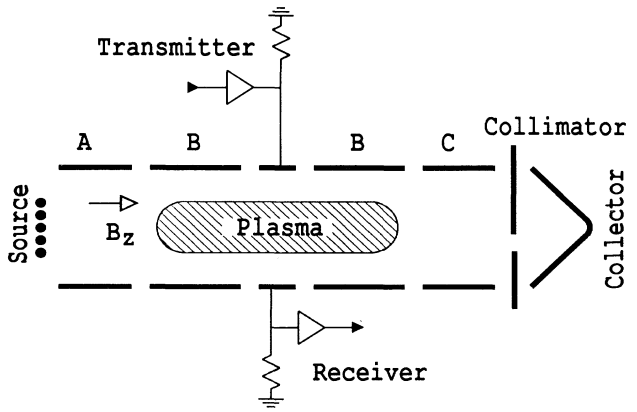

FIG. 1. Schematic diagram of the cylindrical containment system.

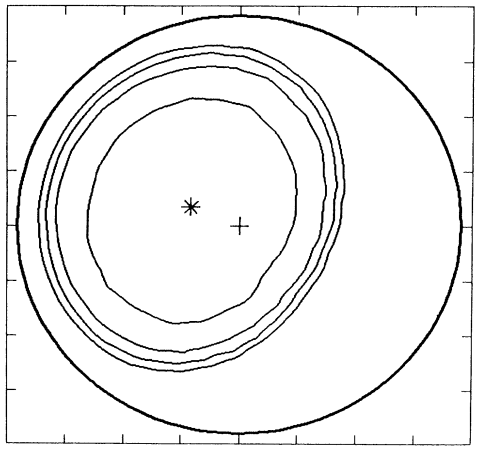

FIG. 2. Equally spaced contours of z-averaged density $n(r,\theta)$ measured phase coherent with a large-amplitude $l=1$ diocotron wave. The outer circle represents the cylindrical wall, the cross the location of the wall center, and the asterisk the center of mass of the plasma. Tick marks are at 1-cm intervals.

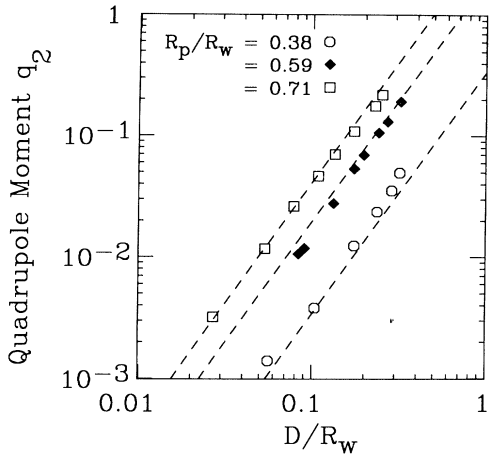

FIG. 3. Measured plasma distortion vs amplitude for plasmas of three different radii. Dashed lines graph Eq. (2).

the mode amplitude. The charges revolve due to $\mathbf{E}\times\mathbf{B}$ drifts at a frequency $f_0=cN_Le/\pi B_zR_w^2$ which depends on the line density $N_L\equiv\int n_0(r)2\pi r\,dr$ and on B_z. Additionally, linear theory predicts small increases in f_0 due to finite length effects.[4] For comparison, the cylindrical plasma rotates about its own center at a frequency $f_R\approx f_0R_w^2/R_p^2$. The linear theory requires $\delta n(r)\ll n_0(r)$.

We believe that this diocotron mode is more accurately described as the entire plasma column displaced off the cylindrical axis by a distance D, and revolving around this axis due to $\mathbf{E}\times\mathbf{B}$ drift. Of course, for small displacements this can be modeled by the perturbation charges of Eq. (1). However, we find that nonlinear effects appear not when $\delta n\sim n_0$ at some radius, but rather when D becomes comparable to R_w. Two simple effects then give nonlinear frequency shifts: The frequency tends to increase because the plasma column is closer to the image charges in the wall; and the frequency tends to decrease because the plasma column distorts so as to be elongated in the θ direction.

Figure 2 shows contours of the z-integrated plasma density $n(r,\theta)$ measured phase coherent with a large-amplitude diocotron mode at a frequency $f=78.6$ kHz. The mode has been driven to a selected amplitude by positive feedback over a period of a few hundred cycles: The wave signal is received on one wall sector, amplified, phase shifted, and then applied to an opposing wall sector, as shown in Fig. 1. The plasma column is both displaced from the cylindrical axis ($D/R_w=0.23$), and elongated in the θ direction. This plot was constructed from about 10^3 separate inject-manipulate-dump cycles, with a single $n(r,\theta)$ measurement on each cycle. We vary θ by varying the dump time by Δt relative to a zero crossing of the received wave, giving $\theta=2\pi f\Delta t$; and the collimator hole is moved radially to obtain the radial dependence. The density is interpolated between data points, and linearly spaced contours are shown in Fig. 2. The regularity of the density contours reflects the fact that shot-to-shot variations in the measured plasma density at any point are small ($\sim 1\%$).

The plasma elongation can be characterized by the quadrupole moment q_2, which can be calculated from $n(r,\theta)$. We define $q_2\equiv(p_{xx}-p_{yy})/(p_{xx}+p_{yy})$, where $p_{xx}\equiv\int x^2n(x,y)dx\,dy$, with a similar definition for p_{yy}. Here the (x,y) coordinate system is defined to have its origin at the plasma center of mass and x lies along the long axis of the plasma. If an initially circular plasma of radius R_p (defined to be the distance from the plasma center to a point at which the density falls by a factor of $\frac{1}{2}$) is elongated by a small amount Δ in the x direction and shortened by Δ in the y direction, then $q_2\approx\Delta/R_p$. When the plasma is not circular we use the displacement of the center of mass as a measurement of D.

Figure 3 shows the measured quadrupole distortion q_2 vs D for three plasmas of different radii R_p. For each plasma, the distortion scales as D^2, but the amount of distortion also depends upon R_p. We find that our data for eight different radius plasmas (a total of 79 points) is well fitted with

$$q_2=16.2(R_p/R_w)^4(D/R_w)^2, \tag{2}$$

shown as dashed lines in Fig. 3.

This plasma distortion is accompanied by a shift in the mode frequency which also scales as D^2. Figure 4 shows the measured variations in mode frequency for the three plasmas of Fig. 3. The measured small-amplitude frequencies, f_0, are 23.4, 71.9, and 77.9 kHz, in order of increasing plasma radius. The measured frequencies at large amplitude differ from the small-amplitude frequencies as

$$(f-f_0)/f_0=\alpha(D/R_w)^2 \tag{3}$$

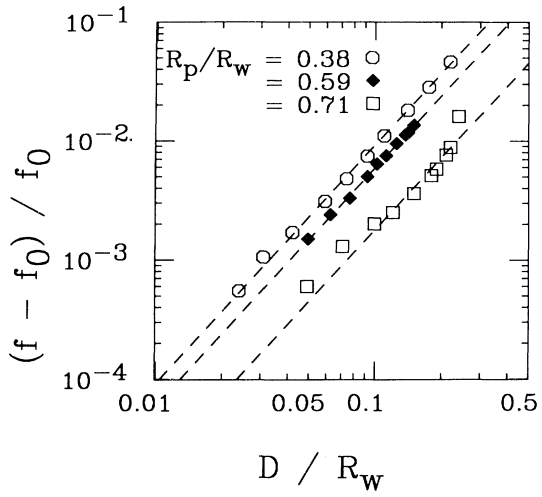

FIG. 4. Measured frequency shift vs amplitude for three different radius plasmas. The dashed lines are fits of the form $\alpha(D/R_w)^2$, giving α=0.92, 0.59, and 0.18.

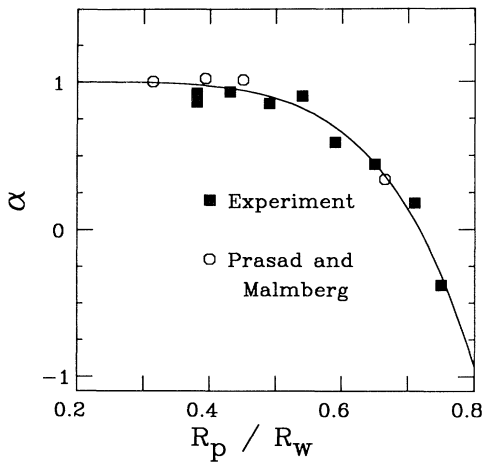

FIG. 5. Measured coefficient of frequency shift [defined by Eq. (3)] vs plasma radius. The solid line graphs Eq. (4). Also shown are the results of a computer calculation by Prasad and Malmberg based upon their theory.

up to very large displacements. As can be seen in Fig. 4, the coefficient α depends on R_p.

We have measured this large-amplitude frequency shift for a total of eight different size plasmas. The resulting coefficient α defined by Eq. (3) is plotted in Fig. 5. The data are well described by

$$\alpha = 1 - 7.3(R_p/R_w)^6, \tag{4}$$

as shown by the curve.

This nonlinear frequency shift can be understood as being due to two effects: A rigid displacement of the plasma column brings it closer to its image charges in the wall, thereby tending to raise the frequency, and the elongation of the plasma column spreads the image charges in the θ direction, thereby reducing the image electric field and tending to decrease the frequency.

The frequency shift due to a rigid displacement can be found from an elementary calculation. We model the plasma as a charge distribution that is cylindrically symmetric around an axis displaced from the wall axis by D, and with charge per unit length of $-N_L e$. It follows from Gauss's law that the electric field outside the plasma is the same as that of a line charge with the same charge per length located at the plasma center. Using the method of images the wall can be replaced by an image with line charge $+N_L e$ located at a radius of $r = r_w^2/D$. The image field at the wall axis gives the linear $\mathbf{E}\times\mathbf{B}$ frequency f_0, whereas the image field at the center of the displaced plasma gives a frequency f shifted from f_0 by

$$\left.\frac{f-f_0}{f_0}\right|_{\text{displ}} = \frac{1}{1-(D/R_w)^2} - 1 \approx \left(\frac{D}{R_w}\right)^2. \tag{5}$$

This explains the $\alpha = 1$ term of Eq. (4).

The frequency shift due to the plasma distortion can be estimated for a constant-density plasma of radius R_p by considering a quadrupole charge perturbation on the surface of the displaced column. A straightforward calculation shows that to lowest order the image charges create an electric field that lowers the diocotron frequency by an amount

$$\left.\frac{f-f_0}{f_0}\right|_{\text{elong}} = -\frac{1}{2}\left(\frac{R_p}{R_w}\right)^2 q_2 = -8.1\left(\frac{R_p}{R_w}\right)^6\left(\frac{D}{R_w}\right)^2, \tag{6}$$

where we have used Eq. (2) for q_2. These two effects [Eqs. (5) and (6)] give a theoretical $\alpha = 1 - 8.1(R_p/R_w)^6$, in good agreement with the measured α in Eq. (4). As mentioned earlier, finite length effects cause shifts in the linear frequency f_0, but we have no theory for how they should affect the nonlinear shifts that we measure.

Alternately, the distortion of the plasma column and the mode frequency can be calculated from the assumption that potential and density are stationary in the frame rotating at the mode frequency. This implies that density and potential contours are coincident in that frame.[10] We have incorporated this assumption into a computer code that models the plasma as a constant-density "waterbag." The boundary shape and the mode frequency are iterated until the boundary matches a potential contour. We find that this code gives close agreement with the experimental results: The best-fit coefficient for q_2 vs D is 16.7 as compared to 16.2 from experiment [Eq. (2)], and the best-fit coefficient for α vs R_p is 7.6 as compared to 7.3 from experiment [Eq. (4)].

Prasad and Malmberg[10] have developed a perturbation theory based upon the same assumption. Their calculations are in good agreement with experiment at low

amplitudes only, i.e., $D/R_w < 0.1$. Their perturbation theory suffers from the choice of the cylindrical axis as the coordinate center: Large perturbations of high order are needed just to model a displacement of the plasma without distortion. Essentially, their perturbation terms are expansions in D/R_p, whereas we find nonlinear effects entering as $(D/R_w)^2$.

In summary, the $l=1$, $k_z=0$ diocotron mode can be understood as a drift of an off-axis plasma column. At large mode amplitudes the plasma column distorts into an oval shape and the mode frequency shifts. The distortion is determined by the requirement that potential and density contours are coincident in the rotating frame. We have explained the observed variation of mode frequency in terms of a simple model with two effects: (1) The frequency tends to increase when a line charge is closer to its image charge, and (2) the frequency tends to decrease due to the distortion of the column.

We wish to thank S. A. Prasad for providing the computer results displayed in Fig. 5, and for enlightening discussions. We also wish to acknowledge enlightening discussions with Warren White, T. M. O'Neil, and Ralph A. Smith. This work was supported by Office of Naval Research Contract No. N00014-82K0621 and National Science Foundation Grant No. NSF PHY87-06358.

[1]C. A. Kapetanakos, D. A. Hammer, C. D. Striffler, and R. C. Davidson, Phys. Rev. Lett. **30**, 1303 (1973).

[2]O. Buneman, R. H. Levy, and L. M. Linson, J. Appl. Phys. **37**, 3203 (1966).

[3]J. J. Bollinger and D. J. Wineland, Phys. Rev. Lett. **53**, 348 (1984).

[4]S. A. Prasad and T. M. O'Neil, Phys. Fluids **27**, 206 (1984).

[5]J. S. deGrassie and J. H. Malmberg, Phys. Fluids **23**, 63 (1980).

[6]C. F. Driscoll, J. H. Malmberg, and K. S. Fine, Phys. Rev. Lett. **60**, 1290 (1988).

[7]R. J. Briggs, J. D. Daugherty, and R. H. Levy, Phys. Fluids **13**, 421 (1970).

[8]R. H. Levy, Phys. Fluids **11**, 920 (1968).

[9]Ronald C. Davidson, *Theory of Nonneutral Plasmas* (Benjamin, Reading, MA, 1974).

[10]S. A. Prasad and J. H. Malmberg, Phys. Fluids **29**, 2196 (1986).